

SYMMETRY RESTORATION FOR ODD-MASS NUCLEI WITH A SKYRME ENERGY DENSITY FUNCTIONAL *

B. Bally, B. Avez, and M. Bender

Université Bordeaux 1, CNRS/IN2P3, Centre d'Etudes Nucléaires de Bordeaux Gradignan, CENBG, Chemin du Solarium, BP120, F-33175 Gradignan, France

P.-H. Heenen

PNTPM, CP229, Université Libre de Bruxelles, B-1050 Bruxelles, Belgium

In these proceedings, we report first results for particle-number and angular-momentum projection of self-consistently blocked triaxial one-quasiparticle HFB states for the description of odd- A nuclei in the context of regularized multi-reference energy density functionals, using the entire model space of occupied single-particle states. The SIII parameterization of the Skyrme energy functional and a volume-type pairing interaction are used.

1. Introduction

Methods based on the self-consistent mean-field approach provide a set of fully microscopic theoretical tools that can be applied to all bound atomic nuclei in a systematic manner irrespective of their mass, N/Z ratio, and deformation.¹ Pure mean-field methods, however, have several limitations. The first one is due to the determination of a wave function in an intrinsic frame of reference. Although the symmetry-breaking mean-field approach is a very efficient and transparent way to grasp the effect of correlations associated with collective modes in the limit of strong correlations,^{2,3} the absence of good quantum numbers and the corresponding selection rules compromises the calculation of transition moments. For example, broken rotational symmetry mixes states with different eigenvalues of \hat{J}^2 , i.e. the members of a rotational band, and independent quasiparticle states of BCS type used to describe pairing correlations are spread over several particle numbers. The second limitation concerns nuclei for which a mean-field description through a single configuration breaks down because several configurations with different shell structure are close in energy. To overcome these limitations requires what is often called "beyond-mean-field methods", i.e. symmetry restoration and configuration mixing within the Generator Coordinate Method (GCM).^{2,3,4,5}

There are many more applications of mean-field and "beyond" methods to even-even nuclei than there are for odd- A nuclei (not to mention odd-odd ones). The most important reason is that the last nucleon in the odd- A system breaks some of the symmetries that make such methods particularly efficient for even-even systems.

*Based on talk presented at 18th Nuclear Physics Workshop "Maria and Pierre Curie", 2011, Kazimierz, Poland.

2. Odd-mass nuclei in self-consistent mean-field models

Odd-mass nuclei are described as one-quasiparticle states build on a HFB vacuum.² The most transparent way to represent such a state is in the canonical basis $\{a_i^\dagger\}$

$$|q_b\rangle = a_b^\dagger \prod_{i \neq b > 0} (\bar{U}_{ii} + \bar{V}_{i\bar{i}} a_i^\dagger a_{\bar{i}}^\dagger) |-\rangle \quad (1)$$

where i and \bar{i} are the indices of the paired conjugate states, where we use the usual convention $i > 0$ and $\bar{i} < 0$, and b is the index of the blocked single-particle state. The single-particle states and Bogoliubov matrices U and V are determined self-consistently. The corresponding HFB equation is obtained from variation of the energy with the obligatory constraints ensuring that $|q_b\rangle$ remains a quasiparticle vacuum and on proton and neutron number.^{2,3} Optional constraints are on the two components of the quadrupole tensor in the intrinsic major axis system of the triaxial shape and on the angular momentum component I_x along one major axis. As done in our earlier configuration mixing calculations, we add the Lipkin-Nogami prescription to the HFB equations to enforce pairing correlations in all mean-field states.^{6,7} The resulting HFB equations for the blocked state are solved using the "two-basis method", where in an iterative procedure the HFB Hamiltonian is diagonalized in the single-particle basis of eigenstates of the HF Hamiltonian in a coordinate-space representation.⁶

3. Going "beyond the mean field"

Restoring the symmetries decomposes a given SCMF state into states with good quantum numbers. Eigenstates of the particle-number operator \hat{N} with eigenvalue N_0 are obtained applying the particle-number projection operator³

$$\hat{P}_{N_0} = \frac{1}{2\pi} \int_0^{2\pi} d\phi_N e^{i\phi_N(\hat{N}-N_0)} \quad (2)$$

to the SCMF states for protons and neutrons. Eigenstates of the total angular-momentum operator in the laboratory frame \hat{J}^2 and its z component \hat{J}_z with eigenvalues $\hbar^2 J(J+1)$ and $\hbar M$, respectively, are obtained applying the operator³

$$\hat{P}_{MK}^J = \frac{2J+1}{16\pi^2} \int_0^{2\pi} d\alpha \int_0^\pi d\beta \sin(\beta) \int_0^{4\pi} d\gamma \mathcal{D}_{MK}^J(\alpha, \beta, \gamma) \hat{R}(\alpha, \beta, \gamma), \quad (3)$$

where $\hat{R} = e^{-i\alpha\hat{J}_z} e^{-i\beta\hat{J}_y} e^{-i\gamma\hat{J}_z}$ is the rotation operator and \mathcal{D}_{MK}^J a Wigner function. Both depend on the Euler angles α , β , and γ . \hat{P}_{MK}^J picks the component with angular-momentum projection K along the intrinsic z axis from a mean-field state. The projected state is then obtained by summing over all K components

$$|JM\nu q_b\rangle = \sum_{K=-J}^{+J} f_\nu^J(K, q_b) \hat{P}_{MK}^J |q_b\rangle = \sum_{K=-J}^{+J} f_\nu^J(K, q_b) |JMK q_b\rangle \quad (4)$$

with weights $f_\nu^J(K, q_b)$ determined from a variational principle that leads to the so-called Hill-Wheeler-Griffin (HWG) equation^{2,3}

$$\sum_{K'=-J}^{+J} \left(\langle JMKq_b | \hat{H} | JMK'q_b \rangle - E_\nu \langle JMKq_b | JMK'q_b \rangle \right) f_\nu^J(K', q_b) = 0, \quad (5)$$

which for sake of simple notation we write for a Hamilton operator. In practice, we use an effective interaction that is provided by a multi-reference (MR) energy density functional (EDF). It is the generalization of the single-reference (SR) EDF employed in SCMF methods to calculate the non-diagonal kernels entering the symmetry-restored energy and the HWG equation (5). It is usually postulated in a form that preserves analogies with the case of a Hamilton operator.^{8,9,10} However, the MR EDF has to be regularized to remove spurious contributions to the energy that manifest themselves through divergences and/or finite steps when plotting the symmetry-restored energy as a function of a collective coordinate.^{11,12} We have implemented such regularization^{13,14} into our codes for general configuration mixing.¹⁵ We use the parameterization SIII¹⁶ of the Skyrme EDF together with a contact pairing interaction of volume type and a strength of 300 MeV fm³ together with cutoffs at 5 MeV above and below the Fermi energy.⁷ The Coulomb exchange term is neglected as done in our earlier regularized MR EDF calculations.^{12,13} The non-diagonal norm kernels entering the symmetry-restored HWG equation (5) are calculated directly with their sign in a technique based on a Pfaffian.

4. An illustrative example: ⁴⁹Cr

We have chosen ⁴⁹Cr for a first exploratory study as it exhibits several low-lying collective rotational bands that can be easily associated with particular blocked single-particle levels. A detailed study of the adjacent even-even ⁴⁸Cr that allows for the analysis of the change brought by the additional nucleon is also underway.

4.1. Projected energy surfaces

The first step of our calculation was to determine which quasiparticle gives the lowest energy at the Single-Reference level. It is a quasiparticle with parity minus and with the mean value of the projection along the deformation axis of the angular momentum close to $\frac{5}{2} : \langle J_3 \rangle^\pi \approx 2.5^-$, which agrees with the experimental finding for the ground state that has $J^\pi = \frac{5}{2}^-$. We then tried to follow this quasiparticle in the first sextant of the $\beta - \gamma$ plane. As we have neither good J nor good J_3 , however, it is not always clear which quasiparticle should be blocked. This ambiguity presents an additional motivation to go to the Multi-Reference level, that is to restore the angular momentum. As demonstrated for example by Schunck *et al.*,¹⁸ because of the time-odd components in the EDF the sextants are not equivalent, and a full study would require to explore at least three out of the six. Test calculations in the other sextants indicate, however, that for this blocked quasiparticle

the differences after K mixing remain tiny, and do not have any importance for the present discussion. This might not be the case for other blocked quasiparticles, and certainly there will be significant differences between the sextants when cranking the quasiparticle states to higher spin.

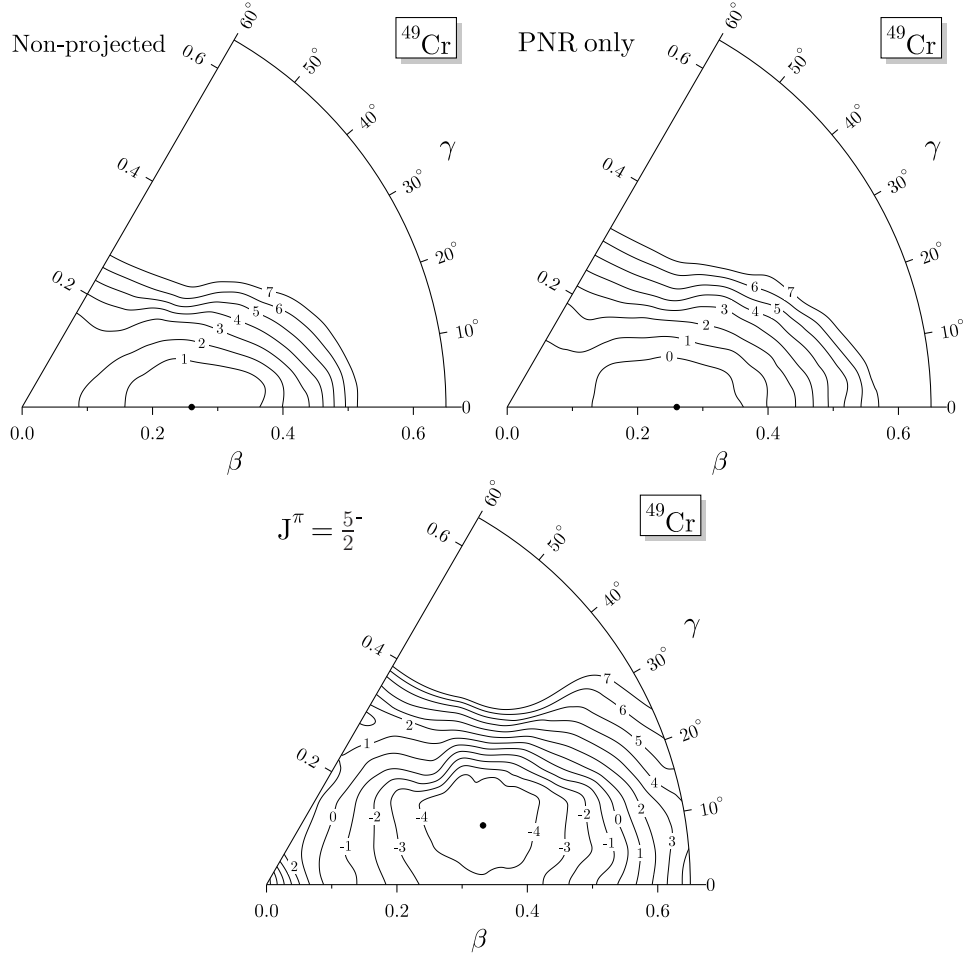


Fig. 1. Top left: Non-projected energy surface, in the first sextant of the $\beta - \gamma$ plane, of the lowest one-quasiparticle state with $\langle J_3 \rangle^\pi \approx 2.5^-$ in ^{49}Cr . Top right: Particle-number restored energy surface constructed from the same one-quasiparticle states. Bottom: Particle-number and angular-momentum restored energy surface for the lowest $J^\pi = \frac{5}{2}^-$, based again on the same one-quasiparticle states. Energies are normalized to the minimum of the non-projected surface. The deformation parameter $\beta = \sqrt{\frac{5}{16} \frac{4\pi}{3R^2A}} \langle Q_2 \rangle$ with $R \equiv 1.2A^{1/3}$ fm and γ are those of the (non-projected) intrinsic states.

In the top left of Fig. 1 is plotted the non-projected energy surface up to 7

MeV. The energy is normalized to the minimum we found and which turns out to be axial ($\beta = 0.26$, $\gamma = 0.0^\circ$). In the top right of Fig. 1 we present the particle number restored (PNR) energy surface, where the projected energies are plotted at the deformation of the SCMF states they have been obtained from.^a One observes that the PNR does not change the global shape of the surface. In particular, the minimum remains axial. The PNR gives an almost constant overall energy gain of about 1 MeV for the entire surface. When projecting on both particle number and angular momentum, we get for $J = \frac{5}{2}$, the J which gives the absolute minimum after projection, the surface plotted in the bottom of Fig. 1. And as one can see, the topography of the surface has dramatically changed: the minimum has moved into triaxiality ($\beta = 0.33$, $\gamma = 15.3^\circ$), and the surface is now centered around this minimum, which is about 5 MeV lower than the non-projected one. The angular-momentum projected surface is thus more rigid against oblate deformation than the non-projected one.

In Fig. 2 we compare the $J^\pi = \frac{5}{2}^-$ energy surface of ^{49}Cr (left), now renormalized to its minimum, with the $J^\pi = 0^+$ energy surface of ^{48}Cr (right), also normalized to its minimum. One immediately sees that the deepest part of the surface is very similar in both cases, in particular the minimum does not move much by the addition of one extra nucleon to ^{48}Cr . By contrast, the energy surface of the $J^\pi = \frac{5}{2}^-$ in ^{49}Cr is clearly more rigid than the $J=0^+$ surface in ^{48}Cr , i.e. for the former the energy grows faster when moving away from the minimum. It will be interesting to see if these remarks remain true for different J coming from other blocked quasiparticles.

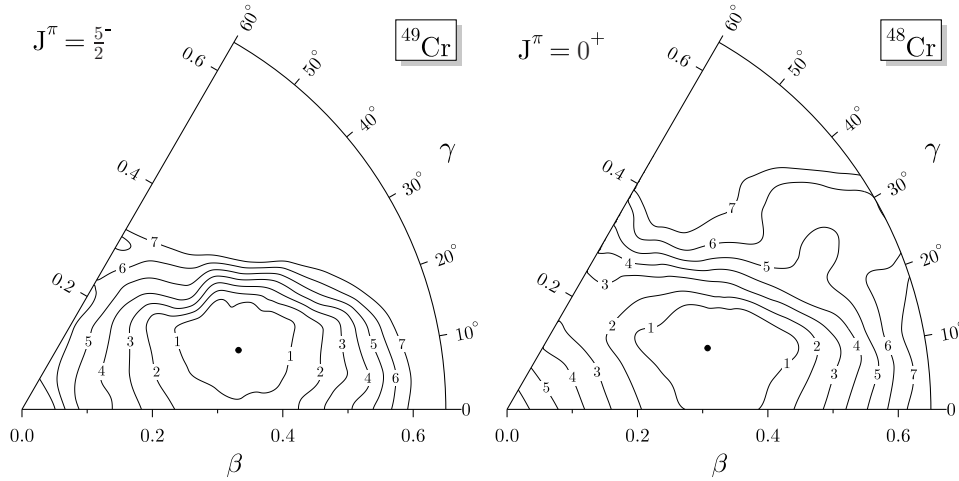


Fig. 2. Left: Energy surface, in the first sextant of the $\beta - \gamma$ plane, of the lowest $J^\pi = \frac{5}{2}^-$ after K mixing in ^{49}Cr . Right: Same for the lowest $J^\pi = 0^+$ in ^{48}Cr . Energies are normalized to the minimum of each surface, which is marked by a filled circle.

^aThe same representation is also adopted for the angular-momentum restored surfaces.

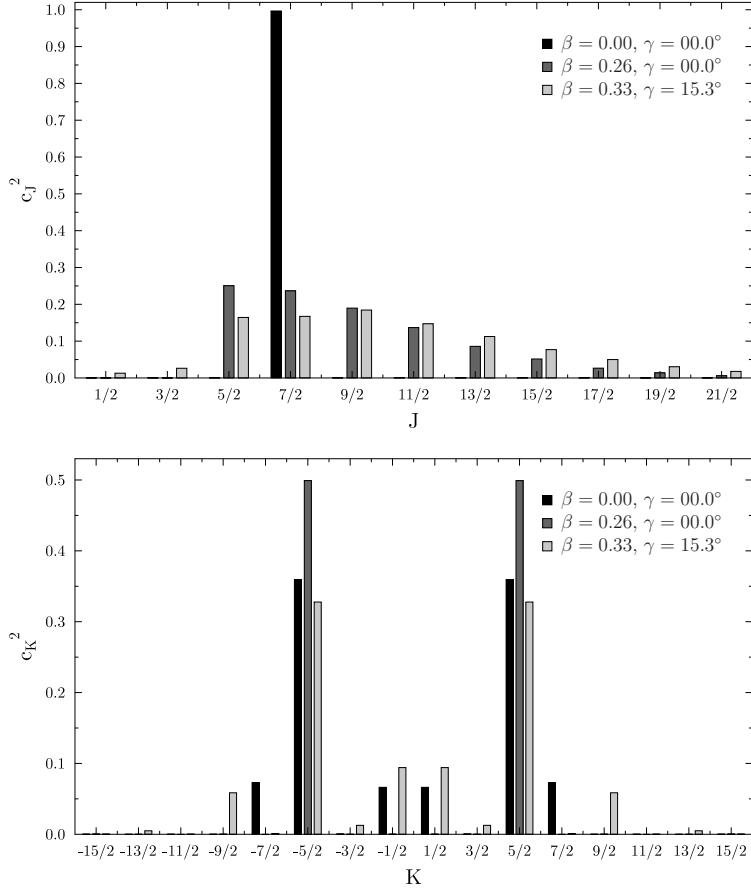


Fig. 3. Top: square of the weights of the different J components summed over K , for three different deformations. Bottom: same but for the weights of the K components summed over J .

4.2. J and K decompositions of SCMF states

In order to better understand how the projection of quasiparticle states works, it is illuminating to look at the decomposition of SCMF states on different angular momenta J and their intrinsic components K . We plot in Fig. 3 the square of the weights of J and K components for several points in the β - γ plane with different deformation. If one looks first at the axially constrained point that corresponds to the minimum before projection (dark grey bars in Fig. 3), one sees that there is indeed not just one J , but a full distribution beginning at $J = \frac{5}{2}$, which is the largest component in the distribution, and decreasing with increasing J . Together with the gain in energy, the fact that there are different J components in the SCMF state proves a posteriori the need for angular-momentum projection. One also notes that

there is no component with $J = \frac{1}{2}$ or with $J = \frac{3}{2}$. This can be understood when looking at the K decomposition of this state. Here, one can see that there are only two different K components, $K = \frac{5}{2}$ and its partner^b $K = -\frac{5}{2}$. As K has to be less than or equal to J , the $J = \frac{1}{2}$ and $J = \frac{3}{2}$ components vanish. It is also interesting to note that even if we don't have axial symmetry, a state constrained to axial deformation of its local density has in first approximation a good K .

The light grey bars of Fig. 3 represent the J and K decomposition of the state which gives the triaxial minimum after projection on $J = \frac{5}{2}$. As one can see, the distribution has changed: it is now the $J = \frac{9}{2}$ component which is the largest, and the distribution is more evenly divided around this maximum. But more importantly, the K decomposition one has now not only $K = \pm\frac{5}{2}$, but a distribution of K with a staggering which favors $K = \pm\frac{1}{2}, \pm\frac{5}{2}, \pm\frac{9}{2} \dots$. So even if $K = \pm\frac{5}{2}$ remains the largest component in this distribution, this points out the necessity for a K mixing as presented in Eqns. (4) and (5).

Finally, the black bars in Fig. 3 represent the J and K decomposition of a state constrained to a spherical density distribution. One notices that there is only a $J = \frac{7}{2}$ component in the decomposition. This can be easily understood: imposing spherical density, the single-particle wave functions are almost eigenstates of angular momentum, such that the HFB state is also almost an eigenstate of J , with the eigenvalue determined by the j of the blocked particle, which in this case is in the $f_{7/2}$ shell. By contrast, nothing in our calculation fixes which magnetic substate in the $f_{7/2}$ shell is blocked. As a consequence, we find an arbitrary combination that depends mainly on the initialization of the blocked HFB calculation.

5. Summary and Outlook

We have reported first results obtained from a method that describes properties of odd- A nuclei by particle-number and angular-momentum projected configuration mixing based of self-consistently blocked one-quasiparticle states and using the Skyrme EDF.

We focussed here on symmetry restoration in a regularized MR-EDF framework. A symmetry-restored GCM calculation along the same lines is underway and will be reported elsewhere.¹⁹ Having a method that allows to treat odd- A and even-even nuclei on the same footing provides a versatile tool for numerous studies of nuclear structure, such as the coupling of single-particle and shape degrees of freedom, the analysis of signatures for shell structure such as separation energies, g factors, spectroscopic quadrupole moments, and their evolution with N and Z , or the analysis of the interplay of pairing correlations and fluctuations in shape degrees of freedom for the odd-even mass staggering.

^bFinding components of equal weight for $\pm K$ is a consequence of our choice of having eigenstates of the x signature operator: $\hat{R}_x = e^{-i\pi\hat{J}_x}$.

Acknowledgments

This research was supported in parts by the Agence Nationale de la Recherche under Grant No. ANR 2010 BLANC 0407 "NESQ", by the IN2P3/CNRS through the PICS No. 5994, and the PAI-P6-23 of the Belgian Office for Scientific Policy. The computations were performed using HPC resources from GENCI-IDRIS (Grant 2011-050707). BB also thanks for travel support by LEA-COPIGAL.

References

1. M. Bender, P.-H. Heenen, P.-G. Reinhard, *Rev. Mod. Phys.* **75** (2003) 121.
2. P. Ring and P. Schuck, *The Nuclear Many-Body Problem*, (Springer, New York, Heidelberg, Berlin, 1980).
3. J. P. Blaizot and G. Ripka, *Quantum theory of finite systems* (MIT, Cambridge, 1986).
4. J. L. Egido and L. M. Robledo, *Lect. Notes Phys.* **641** (Springer, Berlin, 2004), 269.
5. M. Bender, *Eur. Phys. J.* **ST156** (2008) 217.
6. B. Gall *et al.*, *Z. Phys. A* **348** (1994) 183.
7. C. Rigollet, P. Bonche, H. Flocard, and P.-H. Heenen, *Phys. Rev. C* **59** (1999) 3120.
8. P. Bonche *et al.*, *Nucl. Phys. A* **510** (1990) 466.
9. R. R. Rodríguez-Guzmán *et al.*, *Nucl. Phys. A* **709** (2002), 201.
10. L. M. Robledo, *Int. J. Mod. Phys. E* **16** (2007) 337.
11. D. Lacroix, T. Duguet, and M. Bender, *Phys. Rev. C* **79** (2009) 044318.
12. M. Bender, T. Duguet, and D. Lacroix, *Phys. Rev. C* **79** (2009) 044319.
13. M. Bender, T. Duguet, P.-H. Heenen, D. Lacroix, *Int. J. Mod. Phys. E* **20** (2011) 259.
14. M. Bender, B. Avez, T. Duguet, P.-H. Heenen, and D. Lacroix, *in preparation*.
15. M. Bender and P.-H. Heenen, *Phys. Rev. C* **78** (2008) 024309.
16. M. Beiner *et al.*, *Nucl. Phys.* **A238** (1975) 29.
17. B. Avez and M. Bender, preprint arXiv:1109.2078 v1.
18. N. Schunck *et al.*, *Phys. Rev. C* **81** (2010) 024316.
19. B. Bally, B. Avez, M. Bender, and P.-H. Heenen, *in preparation*.